Conserved gene clusters in the scrambled plastomes of IRLC legumes (Fabaceae: Trifolieae and Fabeae).

Saemundur Sveinsson[1*], Quentin Cronk[2]

[1]Faculty of Land and Animal Resources, Agricultural University of Iceland, Keldnaholt, 112 Reykjavik, Iceland;[2]Department of Botany and Biodiversity Research Centre, University of British Columbia, 6270 University Boulevard, Vancouver BC V6T 1Z4, Canada.

Author for correspondence:

Saemundur Sveinsson

Tel: 354-4335219

Email: saemundur@lbhi.is

Total word count (excluding summary, references and legends):	2884	No. of figures:	3 (Figs 1 and 2 in colour)
Summary:	179	No. of Tabels:	3
Introduction:	397	No. of Supporting Information files:	0
Materials and Methods:	1038		
Results:	663		
Discussions:	719		
Acknowledgements:	61		

17 Summary

18 The plastid genome retains several features from its cyanobacterial-like ancestor, one being
19 the co-transcriptional organization of genes into operon-like structures. Some plastid operons
20 have been identified but undoubtedly many more remain undiscovered. Here we utilize the
21 highly variable plastome structure that exists within certain legumes of the inverted repeat
22 lost clade (IRLC) to find conserved gene clusters. These plastomes exhibit an unusually high
23 frequency of translocations and inversions. We analysed the plastomes of 23 legume species
24 and identified 32 locally collinear blocks (LCBs), which are regions within the plastid
25 genomes that occur in different orientation and/or order among the plastid genomes but are
26 themselves free from internal rearrangements. Several represent gene clusters that have
27 previously been recognized as plastid operons. It appears that the number of LCBs has
28 reached saturation in our data set, suggesting that these LCBs are not random, but likely
29 represent legume plastid operons protected from internal rearrangement by functional
30 constraint. Some of the LCBs we identify, such as *psbD*/C/Z, are previously known plastid
31 operons. Others, such as *rpl32-ndhF-psbA-matK-rbcL-atpB-atpE*, may represent novel
32 polycistronic operons in legumes.

33

34 Key words (5-8): Fabeae, IRLC, massively parallel sequencing , plastid operons, plastome
35 evolution, plastome rearrangements, Trifolieae.

36

Introduction

The plastid genome, also known as the plastome, refers to the total genetic information of a single plant organelle, the plastid, which takes many developmental forms, the most notable being the chloroplast (Bock, 2007). Plastid genomes are circular structures of double stranded DNA, usually consisting of about 100-120 genes and are around 120-160 kb long in photosynthesizing plants (Bock, 2007). Their size, structure and gene content are highly conserved across land plants (Wicke *et al.*, 2011). However there are exceptions, such as the Geraniaceae and Campanulaceae, which are two angiosperm families known to contain species with highly rearranged plastomes (Haberle *et al.*, 2008; Guisinger *et al.*, 2011). A dominating feature of plastid genomes is the presence of a large inverted repeat (Wicke *et al.*, 2011; Zhu et al., 2015) separated by a small single copy region that is variable in orientation (Walker et al. 2015). However some plant groups have lost one copy of the repeat, one being a clade within papilionoid legumes (Fabaceae), known as the inverted repeat lost clade (IRLC) (Wojciechowski *et al.*, 2000).

Plants obtained their plastid organelles through an endosymbiosis event with a cyanobacteria-like organism, about 1.5 – 1.6 billion years ago (Margulis, 1970; Hedges *et al.*, 2004). Its bacterial origin gives the plastid genome many prokaryotic features, such as small (70S) ribosomes and the absence of mRNA 3' polyA tails (see Stern *et al.*, 2010 for a review). An additional ancestral feature of the plastid genome is the organization of its coding region into multiple gene clusters, or operons (Sugita & Sugiura, 1996; Sugiura *et al.*, 1998). These gene clusters are stretches of the plastome consisting of several genes that are transcribed into di- or polycistronic units, which are then processed before translation (Stern *et al.*, 2010). Several such clusters have already been identified in the plastid (Adachi *et al.*, 2012; Ghulam *et al.*, 2013; Stoppel & Meurer, 2013).

Several legume genera within the IRLC are known to harbour highly rearranged plastomes, as a result from multiple translocations and/or inversions: *Trifolium* (Cai *et al.*, 2008; Sabir *et al.*, 2014; Sveinsson & Cronk, 2014), *Pisum* (Palmer & Thompson, 1982), *Lathyrus* (Magee *et al.*, 2010), *Lens* and *Vicia* (Sabir *et al.*, 2014). The aim of this study is to analyse these rearrangements in these genera within IRLC, in order to investigate whether they can be used to study the organization of plastid genomes into operons.

Material and Methods

Source of plant material

The plant material for this study came from three sources. First, live plants were collected in the field and transplanted to a glasshouse facility. Secondly, seeds were obtained from a commercial provider, Roger Parsons Sweet Peas (Chichester, UK). Thirdly, seeds were received from the USDA germplasm collection at Pullman, Washington (W6). A full list of germplasm used is given in Table 1. All plants were grown in glasshouse facilities at UBC. In all cases where plants required critical determination they were grown until flowering, and herbarium voucher specimens were then collected (UBC).

Illumina sequencing

Total DNA was extracted from fresh leaf material following a modified version of the CTAB protocol (Doyle & Doyle, 1987). RNase treatments were performed (cat. 19101, QIAGEN, Germantown, MD) and DNA quality was assessed by visual inspections on 1% agarose gels. Illumina sequencing libraries were constructed from high quality DNA, using the NEXTflexTM DNA sequencing kit (100 bp Paired-End reads) (cat: 5140-02, BiooScientific Corp, TX). We followed the manufacturer's protocol and c. 400 bp DNA fragments were size selected using Agencourt AMPure XpTM magnetic beads (cat. A63880, BeckmanCoulter Genomics, MA). Completed libraries were pooled and sequenced on a lane of the Illumina HiSeq-2000 platform.

Plastid genome assemblies and annotation

Trimmomatic v.0.3 (Lohse *et al*., 2012) was used to trim and remove low quality Illumina reads, with the following flags: LEADING:20 TRAILING:20 SLIDINGWINDOW:4:15MINLEN:36. High quality reads were used in all subsequent analysis and singlet reads, i.e. reads without a paired end, were discarded. We used the *de novo* method implemented in CLC Genomic Workbench v.7.0.2 to generate assemblies for each species, using the default settings. Contigs of plastid origin were identified by a BLASTN search (Altschul *et al*., 1997) to a plastid genome of a closely related species. These were generally the largest and most high coverage contigs in the *de novo* assembly and always had an E-value of 0 when blasted to the reference plastome. Regions with nucleotides

scored as Ns were manually resolved by retrieving sequence information directly from the quality-trimmed reads. For most species, the *de novo* assembly returned a single large plastid contig. When needed, multiple contigs containing plastid sequence were joined by hand, using information from the quality-trimmed reads. The quality of each plastome assembly was verified by visually by inspecting a BWA mem pileup, v. 0.7.5a (Li & Durbin, 2009), of paired end reads using Tablet v.1.13.12.17 (Milne *et al*., 2013). We made sure that the connections between manually joined contigs were supported by paired-end read mapping. Finally all plastome assemblies were annotated using DOGMA (Wyman *et al*., 2004).

Phylogenetic analysis

Due to the extensive rearrangements observed in the plastomes (see Sabir *et al*., 2014; Sveinsson & Cronk, 2014), we restricted our plastome phylogenetic analysis to protein coding genes. We used a custom phylogenetic pipeline, plast2phy, that extracted protein coding regions from DOGMA annotated plastomes, aligned individual gene with Mafft v. 7.0.5(-auto flag) (Katoh & Standley, 2013), trimmed alignment gaps using trimAl v.1.2 (-automated1 flag) (Capella-Gutiérrez *et al*., 2009) and finally generated a concatenated alignment of all genes. The pipeline, Plast2phy, written in Python, is available at https://github.com/saemi/plast2phy. Model of base substitution were tested for the concatenated matrix using jModelTest v.2.1.1 (Guindon & Gascuel, 2003; Darriba *et al*., 2012). Using the Akaike information criterion (AIC), we determined the GTR+G+I model optimal for the concatenated plastome alignment. We analysed the dataset under maximum likelihood (ML; Felsenstein, 1973) using GARLI (Zwickl, 2006). We ran GARLI v. 2.0 with default settings, using ten independent searches and 100 bootstrap replicates. Bootstrap consensus was calculated using SumTrees v. 3.3.1 in the DendroPy package (Sukumaran & Holder, 2010). Trees from phylogenetic analysis were drawn using FigTree v.1.4.0 (http://tree.bio.ed.ac.uk/software/figtree/), rooted with *Cicer aretinum*.

Identification of locally collinear blocks (LCBs) in plastid genomes

The progressive alignment method, implemented in the MAUVE v.2.3.1 package (Darling *et al*., 2010), was used with the default parameters to identify locally collinear blocks (LCBs) among the plastid genomes listed in Table 1. In this study, a LCB represents a region within a plastid genome that can occur in different orientation and/or order among the studied plastid

genomes, but is free from any internal rearrangements (see Darling *et al*., 2010). These regions are therefore putatively orthologous in nature. I used two programs, projectAndStrip and makeBadgerMatrix (downloaded from http://gel.ahabs.wisc.edu/mauve/snapshots/, on 11 November 2014) to generate a LCB boundary file from the MAUVE alignment. The LCB boundary file contained information on where the LCBs start and end in each of the analysed plastome. I used the chickpea plastome (*Cicer arietinum)* [NCBI Reference Sequence NC_011163] (Jansen *et al*., 2008), as the reference plastome. We visualized the observed plastid rearrangements using Circos v.0.66 (Krzywinski *et al.*, 2009), were a custom Python script was to generate Circos input files and executing the program for each of plastid genome (Figs. 1 and 2). Figure 2 was generated by manually combining all the Circos maps with a phylogenetic cladogram using inkscape (www.inkscape.org). Information regarding the size of LCBs and lengths of protein coding genes in Table 2 are based on the reference plastome of *Cicer arietinum* [NC_011163]. Putative unannotated tRNAs were identified using MITOS (Bernt *et al.*, 2013).

Relationship among divergence time and plastid rearrangements

In order to investigate the relationship among species divergence and the number plastid rearrangements, we estimated two relevant parameters in a pairwise manner. Firstly we estimated the reversal distance using GRIMM v. 2.0.1 (Tesler, 2003). Reversal distance is the minimum number of reversal steps for two genomes to become completely syntenic (Tesler, 2003). GRIMM uses the LCB boundary file, described in the previous section, as its input file. Secondly we used the synonymous substitution rate (Ks) between pairs of plastid genomes as an indicator for the divergence between species. Ks values were calculated using MEGA v.6.0 (Tamura *et al.,* 2013), from a concatenated alignment file of the plastid protein genes. Divergence times can be estimated using published estimates of plastid mutation rates, which range from 1.1 – 2.9 silent substitutions per billion years (Wolfe *et al*., 1987). The reversal distance was plotted against divergence time using R v. 3.0.2 (R Core Team, 2014) and ggplot2 (http://ggplot2.org/), and their relationship visualized using a smoothing curve, using the following command: geom_smooth(degree=1, shape=2/3, method='loess', level=.95).

Results

Phylogeny of species with rearranged plastomes

Mapping the plastome architecture onto the phylogenetic tree of the investigated legume species indicates that the plastomes have clearly undergone multiple multiple and rounds of inversions and translocations throughout the tree (Figs. 1, 2a and 2b.) The phylogenetic analysis of the protein coding regions of our completely sequenced plastomes proved useful in resolving the relationships among the studied species (Fig. 2a.). The phylogeny reported here largely confirms previous studies (LPWG 2013) and is consistent with the *Trifolium* phylogeny using the same methods reported previously (Sveinsson & Cronk 2014) and Fabeae (previously reported in Magee *et al.*, 2010). The tree is rooted on *Cicer*, which along with *Medicago*, shows no evidence of plastid rearrangements compared to other IRLC legumes (Supporting Information 1) and, with the exception of the lost inverted repeat (Wojciechowski *et al.*, 2000), their plastomes are collinear with *Lotus japonicus* (Supporting Information 1, Fig. 3).

Many locally collinear blocks (LCBs) correspond to previously reported plastid operons

The entire plastid genome in these species has been broken up multiple times by rearrangement but certain genomic blocks have never been broken up. MAUVE identified a total of 32 localized collinear blocks (LCB) (Fig. 2b) in the 23 analysed plastomes. Out of these 32 LCBs, 26 contained protein-coding genes and one LCB was made up of the plastid rRNA genes (see Table 2). These 26 blocks varied in size and contained gene clusters (GCs) that varied in the number of genes that they encompass (see Table 2). Nine of the blocks (gene clusters) contained only a single gene, five blocks were composed of two genes and the remaining 12 blocks consisted of more than 2 genes. The largest gene cluster (GC) is GC-1, 13.8 kb in length, containing the following genes: *rpl32, ndhF, psbA, matK, rbcL, atpE* and *atpB* (Table 2). The smallest gene cluster detected was GC-8, about 1.2 kb in length, containing only a single gene, *petN.* Many of the gene clusters have previously been recognized as plastid operons (i.e. transcriptional units), such as GC-2, 6, 7, 18, 27 and 31 (see Sugita & Sugiura, 1996). Several other gene clusters share extensive similarities with previously reported plastid operons but can differ in the presence or absence of a single gene, e.g. GC-11, 12 and 21. Gene containing LCBs cover about 98% of the total length of the

192 *Cicer arietinum* plastome. This suggests that the delimitation of these clusters is not random
193 and is under functional constraint (see discussion).

194

195 **The number of plastome rearrangements increases with divergence time, but levels off**
196 We investigated the relationship between species divergence and the number of plastome
197 rearrangements, by plotting sequence evolution against genome rearrangement. Specifically
198 we plotted pairwise synonymous substitution rate (Ks) against pairwise reversal distances
199 (see Fig. 3). The rationale for this analysis was that if formation of new LCBs in the
200 plastomes is constrained by the presence of plastid operons, blocks should increase in number
201 until functional constraint does not allow further break-up of blocks. We find a pattern
202 consistent with this constraint hypothesis. With evolutionary distance (approximating time)
203 rearrangements increase until saturation is reached. When a smoothing curve is fitted through
204 the data, we observe what seems to a strong positive correlation between evolutionary
205 divergence and plastome rearrangements up until about Ks~0.10 where it starts to level off,
206 which relates to about 9 in reversal distance (Fig. 3). If the plastomes were under no
207 functional constraint there would be no obvious reason that the relationship between
208 divergence and reversal distance would level off at that point. Our results suggest that there is
209 functional constraint on the observed plastome rearrangements and its most likely source is
210 the preservation of functional di- and polycistronic plastid transcriptional units (see
211 discussion). This functional constraint appears to place a limit on the number LCBs (Fig. 3),
212 i.e. limit the extent to which blocks of genes can be broken up. The block cannot be further
213 divided, by inversion and translocation, without breaking co-transcriptional units.

214

215 ## Discussion

216 **The rearrangements of plastomes in IRLC legumes**
217 Plastid genomes of analysed *Trifolium* and the Fabeae (*Lens*, *Vicia*, *Pisum* and *Lathyrus*)
218 species are highly rearranged, as a result of multiple rounds of translocations and/or
219 inversions (Fig. 2 and Fig. 2). These rearrangements have previously been reported (Palmer
220 & Thompson, 1982; Cai *et al.*, 2008; Magee *et al.*, 2010; Sabir *et al.*, 2014; Sveinsson &
221 Cronk, 2014). Plastid genomes tend to be quite conserved structurally across land plants (see

Wicke *et al.*, 2011). However, besides these IRLC legumes, there are other well-known exceptions, such as Geraniaceae (Guisinger *et al.*, 2011) and Campanulaceae (Haberle *et al.*, 2008). The plastome rearrangements described here for the Fabeae appear to be most similar to those reported in *Trachelium caeruleum* (Campanulaceae), since they do not involve proliferation of repeated elements, such as in certain *Trifolium* species (Sveinsson & Cronk, 2014) or in the Geraniaceae (Guisinger *et al.*, 2011; Weng *et al.*, 2013). The functional cause of these rearrangements is not known. The stability of plastid genomes is maintained through recombinational mechanisms, which are controlled by a large number of nuclear genes (see Maréchal & Brisson, 2010). The loss of the inverted repeat may be involved in the genome instability but, if so, the relationship is not simple as some IRLC legumes such as *Medicago* and *Cicer* have well conserved typical legume gene orders. Whatever the functional changes that result from this unprecedented genome instability, it is clear that it offers a unique opportunity for the study the organization of inviolable transcriptional units within the plastid genomes of flowering plants. Against a background of extensive genome scrambling, blocks with conserved gene order stand out.

Do conserved blocks in otherwise rearranged plastomes represent operons?

The genespace of plastid genomes is organized into transcriptional units, similar to operons in the genome of their cyanobacterial ancestors (Stern *et al.*, 2010). However it is important to note that despite plastids being of bacterial origin, most aspects of the regulation of plastid gene expression are radically different from bacteria, mainly due to interactions with the nuclear genome (Stern *et al.*, 2010). Nevertheless, it is well established from functional studies that many plastid genes are organized into dicistronic or polycistronic operon-like units, i.e. co-regulated gene blocks, also known as transcriptional units (Sugita & Sugiura, 1996). It is therefore reasonable to assume that any structural rearrangements that would break up these transcriptional units would be detrimental to the plastid and be selected against.

Our results are in agreement with that assumption, as many of the gene clusters that we observe are known plastid polycistronic operons (Table 2 here; and Table 2 in Sugita & Sugiura, 1996). Examples of this are: (i) Gene Cluster 21 (GC-21, Table 2) that seems to correspond to the *psbB* operon, which has been extensively studied (Stoppel & Meurer, 2013); (ii) GC-7 which contains the same genes as the *psbD*/C/Z operon, which has been

characterized in tobacco (Adachi *et al.*, 2012); (iii) GC-28 which contains all the rRNA genes, which are necessary to construct the plastid 70S ribosome. The numerous genes that are not associated with any other and freely translocate independently, are likely to represent single gene transcriptional units, i.e. monocistronic operons. Gene Cluster 1 (*rpl32-ndhF-psbA-matK-rbcL-atpB-atpE*) is of particular interest, as it contains seven cistrons that previously were thought to be transcribed independently (i.e. as monocistronic units) or belong to different operons (see Table 2 in Sugita & Sugiura, 1996). Our results are highly suggestive that that GC-1 is a conserved plastid operon, at least in the legume species analysed here. Six LCBs without any annotated protein-coding or RNA genes were also identified (varying in size between 177 and 689 nt (see Table 2; Supporting Information 2). However, we identified putative unannotated tRNAs in these blocks (Table 2) and so it is possible that they too are under functional constraint.

These results demonstrate that identification of conserved gene clusters in this clade of rapid structural evolution is a powerful way of provide evidence for previously described plastid operons and potentially to find new ones. Such is the extent of the genic reorganization in the sampled species that it may be argued that the persistence of multiple intact gene blocks is implausible unless these units (Table 2) are inviolable as they represent the fundamental regulatory architecture of the legume plastid.

Acknowledgements

We thank C. Hefer with computer help, D. Kaplan for greenhouse assistance, the Western Canada Research Grid (Westgrid) for computer facilities, USDA and the Desert Legume project for seeds, A. Kuzmin for assistance with sequencing library prep. The work was funded by the Natural Sciences and Engineering Research Council of Canada (NSERC) Discovery Grants Program (grant no. RGPIN-2014-05820 grant to QC).

References

Adachi Y, Kuroda H, Yukawa Y, Sugiura M. **2012**. Translation of partially overlapping *psbD-psbC* mRNAs in chloroplasts: the role of 5'-processing and translational coupling. *Nucleic Acids Research* **40**: 3152–8.

Altschul SF, Madden TL, Schäffer AA, Zhang J, Zhang Z, Miller W, Lipman DJ. **1997**. Gapped BLAST and PSI-BLAST: a new generation of protein database search programs. *Nucleic Acids Research* **25**: 3389–3402.

Bernt M, Donath A, Jühling F, Externbrink F, Florentz C, Fritzsch G, Pütz J, Middendorf M, Stadler PF. 2013. MITOS: Improved de novo Metazoan Mitochondrial Genome Annotation. *Molecular Phylogenetics and Evolution* **69**: 313-319.

Bock R. 2007. Structure, function, and inheritance of plastid genomes. In: Bock R, editor. *Cell and Molecular Biology of Plastids*. Berlin, Germany: Springer, 29–63.

Cai Z, Guisinger M, Kim H-G, Ruck E, Blazier JC, McMurtry V, Kuehl J V, Boore J, Jansen RK. **2008**. Extensive reorganization of the plastid genome of *Trifolium subterraneum* (Fabaceae) is associated with numerous repeated sequences and novel DNA insertions. *Journal of Molecular Evolution* **67**: 696–704.

Capella-Gutiérrez S, Silla-Martínez JM, Gabaldón T. **2009**. trimAl: a tool for automated alignment trimming in large-scale phylogenetic analyses. *Bioinformatics* **25**: 1972–1973.

Darling AE, Mau B, Perna NT. **2010**. Progressivemauve: Multiple genome alignment with gene gain, loss and rearrangement. *PLoS ONE* **5**. e11147.

Darriba D, Taboada GL, Doallo R, Posada D. **2012**. jModelTest 2: more models, new heuristics and parallel computing. *Nature Methods* **9**: 772.

Doyle JJ, Doyle JL. **1987**. A rapid DNA isolation procedure for small quantities of fresh leaf tissue. *Phytochemical Bulletin* **19**: 11–15.

Felsenstein J. **1973**. Maximum likelihood and minimum-steps methods for estimating evolutionary trees from data on discrete characters. *Systematic Zoology* **22**: 240–249.

306 **Ghulam MM, Courtois F, Lerbs-Mache S, Merendino L**. **2013**. Complex processing
307 patterns of mRNAs of the large ATP synthase operon in *Arabidopsis* chloroplasts. *PLoS ONE*
308 **8**: e78265.

309 **Grabherr MG, Haas BJ, Yassour M, Levin JZ, Thompson D a, Amit I, Adiconis X, Fan**
310 **L, Raychowdhury R, Zeng Q, *et al.* 2011**. Full-length transcriptome assembly from RNA-
311 Seq data without a reference genome. *Nature Biotechnology* **29**: 644–652.

312 **Guindon S, Gascuel O**. **2003**. A simple, fast, and accurate algorithm to estimate large
313 phylogenies by maximum likelihood. *Systematic Biology* **52**: 696–704.

314 **Guisinger MM, Kuehl J V, Boore JL, Jansen RK**. **2011**. Extreme reconfiguration of
315 plastid genomes in the angiosperm family Geraniaceae: rearrangements, repeats, and codon
316 usage. *Molecular Biology and Evolution* **28**: 583–600.

317 **Haberle RC, Fourcade HM, Boore JL, Jansen RK**. **2008**. Extensive rearrangements in the
318 chloroplast genome of *Trachelium caeruleum* are associated with repeats and tRNA genes.
319 *Journal of Molecular Evolution* **66**: 350–361.

320 **Hedges SB, Blair JE, Venturi ML, Shoe JL**. **2004**. A molecular timescale of eukaryote
321 evolution and the rise of complex multicellular life. *BMC Evolutionary Biology* **4**: 2.

322 **Jansen RK, Wojciechowski MF, Sanniyasi E, Lee SB, Daniell H**. **2008**. Complete plastid
323 genome sequence of the chickpea (*Cicer arietinum*) and the phylogenetic distribution of
324 *rps12* and *clpP* intron losses among legumes (*Leguminosae*). *Molecular Phylogenetics and*
325 *Evolution* **48**: 1204–1217.

326 **Katoh K, Standley DM**. **2013**. MAFFT Multiple Sequence Alignment Software Version 7:
327 Improvements in Performance and Usability. *Molecular Biology and Evolution* **30**: 772–780.

328 **Krzywinski M, Schein J, Birol I, Connors J, Gascoyne R, Horsman D, Jones SJ, Marra**
329 **MA**. **2009**. Circos: an information aesthetic for comparative genomics. *Genome Research* **19**:
330 1639–1645.

331 **LPWG (The Legume Phylogeny Working Group). 2013**. Legume phylogeny and
332 classification in the 21st century : Progress, prospects and lessons for other species-rich
333 clades. *Taxon* **62**: 217–248.

334 **Li H, Durbin R**. **2009**. Fast and accurate short read alignment with Burrows-Wheeler
335 transform. *Bioinformatics* **25**: 1754–1760.

Li L, Stoeckert CJ, Roos DS. **2003**. OrthoMCL: identification of ortholog groups for eukaryotic genomes. *Genome Research* **13**: 2178–2189.

Liu L, Yu L, Pearl DK, Edwards S V. **2009**. Estimating species phylogenies using coalescence times among sequences. *Systematic Biology* **58**: 468–477.

Liu L, Yu L. **2010**. Phybase: an R package for species tree analysis. *Bioinformatics* **26**: 962–963.

Lohse M, Bolger AM, Nagel A, Fernie AR, Lunn JE, Stitt M, Usadel B. **2012**. RobiNA: a user-friendly, integrated software solution for RNA-Seq-based transcriptomics. *Nucleic Acids Research* **40**: W622–627.

Magee AM, Aspinall S, Rice DW, Cusack BP, Sémon M, Perry AS, Stefanović S, Milbourne D, Barth S, Palmer JD, *et al.* 2010. Localized hypermutation and associated gene losses in legume chloroplast genomes. *Genome Research* **20**: 1700–1710.

Maréchal A, Brisson N. **2010**. Recombination and the maintenance of plant organelle genome stability. *The New Phytologist* **186**: 299–317.

Margulis L. 1979. Origin of Eukaryotic Cells. New Haven, CT, USA: Yale University Press.

Milne I, Stephen G, Bayer M, Cock PJA, Pritchard L, Cardle L, Shaw PD, Marshall D. **2013**. Using Tablet for visual exploration of second-generation sequencing data. *Briefings in Bioinformatics* **14**: 193–202.

Palmer JD, Thompson WF. **1982**. Chloroplast DNA rearrangements are more frequent when a large inverted repeat sequence is lost. *Cell* **29**: 537–550.

R Core Team. **2014**. R: A language and environment for statistical computing. R Foundation for Statistical Computing. Vienna, Austria: R Foundation for Statistical Computing. [WWW document] URL http://www.R-project.org/ [accessed 23 October 2014].

Sabir J, Schwarz E, Ellison N, Zhang J, Baeshen NA, Mutwakil M, Jansen R, Ruhlman T. **2014**. Evolutionary and biotechnology implications of plastid genome variation in the inverted-repeat-lacking clade of legumes. *Plant Biotechnology Journal* **12**: 743–754.

Stamatakis A. **2014**. RAxML version 8: A tool for phylogenetic analysis and post-analysis of large phylogenies. *Bioinformatics* **30**: 1312–1313.

364 **Stern DB, Goldschmidt-Clermont M, Hanson MR**. **2010**. Chloroplast RNA metabolism.
365 *Annual Review of Plant Biology* **61**: 125–155.

366 **Stoppel R, Meurer J**. **2013**. Complex RNA metabolism in the chloroplast: an update on the
367 *psbB* operon. *Planta* **237**: 441–449.

368 **Sugita M, Sugiura M**. **1996**. Regulation of gene expression in chloroplasts of higher plants.
369 *Plant Molecular Biology* **32**: 315–326.

370 **Sugiura M, Hirose T, Sugita M**. **1998**. Evolution and mechanism of translation in
371 chloroplasts. *Annual Review of Genetics* **32**: 437–459.

372 **Sukumaran J, Holder MT**. **2010**. DendroPy: a Python library for phylogenetic computing.
373 *Bioinformatics* **26**: 1569–1571.

374 **Sveinsson S, McDill J, Wong GKS, Li J, Li X, Deyholos MK, Cronk QCB**. **2014**.
375 Phylogenetic pinpointing of a paleopolyploidy event within the flax genus (*Linum*) using
376 transcriptomics. *Annals of Botany* **113**: 753–761.

377 **Sveinsson S, Cronk Q**. **2014**. Evolutionary origin of highly repetitive plastid genomes within
378 the clover genus (*Trifolium*). *BMC Evolutionary biology* **14**: 228.

379 **Tamura K, Stecher G, Peterson D, Filipski A, Kumar S**. **2013**. MEGA6: Molecular
380 Evolutionary Genetics Analysis version 6.0. *Molecular Biology and Evolution* **30**: 2725–
381 2729.

382 **Tesler G**. **2003**. Efficient algorithms for multichromosomal genome rearrangements. *Journal*
383 *of Computer and System Sciences* **65**: 587–609.

384 **Walker JF, Jansen RK, Zanis MJ, Emery NC.** 2015. Sources of inversion variation in the
385 small single copy (SSC) region of chloroplast genomes. *American Journal of Botany*.

386 **Wasmuth JD, Blaxter ML**. **2004**. prot4EST: translating expressed sequence tags from
387 neglected genomes. *BMC Bioinformatics* **5**: 187.

388 **Weng M-L, Blazier JC, Govindu M, Jansen RK**. **2013**. Reconstruction of the ancestral
389 plastid genome in Geraniaceae reveals a correlation between genome rearrangements, repeats
390 and nucleotide substitution rates. *Molecular Biology and Evolution*: 1–15.

Wicke S, Schneeweiss GM, dePamphilis CW, Müller KF, Quandt D. **2011**. The evolution of the plastid chromosome in land plants: gene content, gene order, gene function. *Plant Molecular Biology* **76**: 273–297.

Wojciechowski, M. F., M. J. Sanderson, K. P. Steele, and A. Liston. 2000. Molecular phylogeny of the "temperate herbaceous tribes" of papilionoid legumes: a supertree approach. In: Herendeen PS, Bruneau A, eds. *Advances in Legume Systematics*. Kew, UK: Royal Botanic Gardens, 277-298.

Wolfe KH, Li WH, Sharp PM. **1987**. Rates of nucleotide substitution vary greatly among plant mitochondrial, chloroplast, and nuclear DNAs. *Proceedings of the National Academy of Sciences of the United States of America* **84**: 9054–9058.

Wyman SK, Jansen RK, Boore JL. **2004**. Automatic annotation of organellar genomes with DOGMA. *Bioinformatics* **20**: 3252–3255.

Zhu A, Guo W, Gupta S, Fan W, Mower JP. 2015. Evolutionary dynamics of the plastid inverted repeat: the effects of expansion, contraction, and loss on substitution rates. *New Phytologist.*

Zwickl DJ. **2006**. *Genetic algorithm approaches for the phylogenetic analysis of large biological sequence datasets under the maximum likelihood criterion*. PhD thesis, University of Texas, Austin, TX, USA.

436 Table 1. Information regarding the plastid genomes used in this study. Details regarding the
437 Illumina sequencing and voucher details are presented where applicable. An asterisk (*)
438 indicates species sequenced in this study.

Species (USDA seed accession)	**GenBank accession**	**Herbarium voucher (UBC[2])**
Cicer arietinum L. (NA)	NC_011163	NA
Medicago truncatula Gaertn. (NA)	NC_003119	NA
**Trifolium strictum* L. (PI 369147)	KJ788292	V241491
T. grandiflorum Schreb. (NA)	NC_024034	NA
T. aureum Pollich (NA)	NC_024035	NA
**T. boisseri* Guss. (PI 369022)	KJ788284	V241490
**T. glanduliferum* Boiss. (PI 296666)	KJ788285	V241492
**Vicia sativa* L. (PI 293436)	KJ850242	NA
**Lens culinaris* Medik. (PI 592998)	KJ850239	NA
**Pisum sativum* L. (W6 32866)	KJ806203	V241498
**Lathyrus clymenum* L. (RP[3])	KJ850235	V241501
**L. tingitanus* L. (RP[3])	KJ850238	V241502
L. sativus L. (NA)	NC_014063	NA
**L. odoratus* L. (RP[3])	KJ850237	V241503

**L. pubescens* Hook. & Arn. (RP[3])	KJ806200	V241505
**L. inconspicuus* L. (W6 2817)	KJ850236	V241504
**L. davidii* Hance (RP[3])	KJ806192	V241506
**L. palustris* L. (NA)	KJ806198	V241511
**L. japonicus* Willd.(NA)	KJ806194	NA
**L. littoralis* Endl.(NA)	KJ806197	NA
**L. graminifolius* (S.Watson) T.G.White (DLP[4] accession: 920239)	KJ806193	V241507
**L. ochroleucus* Hook. (NA)	KJ806199	V241489
**L. venosus* Muhl. ex Willd. (NA)	KJ806202	V241509

[1]SD: Standard Deviation

[2]UBC Herbarium, Vancouver BC Canada

[3]Roger Parsons Sweet Peas, Chichester UK

[4]Desert Legume Project Germplasm, AZ USA

445 Table 2. Details regarding the gene content, positional boundaries, length of locally collinear
446 blocks identified within the analysed plastome. An asterisk (*) marks putative tRNAs
447 unannotated in the *Cicer* plastome.

LCB ID	**Genes residing in the LCB**	**LCB boundary[2]**	**LCB length (coding %[1])**
GC-01	*rpl32-ndh*F-*psb*A-*mat*K-*rbc*L-*atp*B-*atp*E	121898 - 125304 and 1 - 10457	13,862 (60.0)
GC-02	*ndh*C-*ndh*K-*ndh*J	10458 - 13156	1,524 (56.5)
GC-03	*rps4*	13157 - 15877	606 (22.3)
GC-04	*ycf3*	15878 - 18242	1,977 (83.6)
GC-05	**trn*E, **trn*I	18243 - 18420	177 (-)
GC-06	*psa*A-*psa*B-*rps14*	18421 - 24458	4,761 (78.9)
GC-07	*psb*Z-*psb*C-*psb*D-*psb*M	24459 - 31398	2,778 (40.0)
GC-08	*pet*N	31399 - 32561	96 (8.3)
GC-09	**trn*Q, **trn*F	32562 - 32875	313 (-)
GC-10	**trn*C, **trn*F, **trn*K, **trn*W, **trn*V	32876 - 33397	521 (-)
GC-11	*rpo*B-*rpo*C1	33398 - 40310	6,050 (87.5)
GC-12	*rpo*C2-*rps2-atp*I-*atp*H-*atp*F-*atp*A	40311 - 51303	8,586 (78.1)
GC-13	**trn*Q, **rrn*L, **trn*E, **rrn*L	51304 - 51635	331 (-)
GC-14	*psb*I-*psb*K	51636 - 54492	297 (10.4)
GC-15	*acc*D-*psa*I	54493 - 58824	1,488 (34.4)
GC-16	*cem*A	58825 - 60169	690 (51.3)
GC-17	*pet*A	60170 - 61921	963 (55.0)
GC-18	*psb*J-*psb*L-*psb*F-*psb*E	61922 - 63839	612 (31.9)
GC-19	*pet*L-*pet*G-*psa*J-*rpl33-rps18-rpl20*	63840 - 67436	1,236 (34.4)

GC-20	*5'rps12-clp*P	67437 - 69967	1,578 (52.2)
GC-21	*psb*B-*psb*T-*psb*N-*psb*H-*pet*B-*pet*D	69968 - 75752	4,667 (80.7)
GC-22	*rpo*A-*rps11-rpl36-rps8*	75753 - 79071	1,932 (58.2)
GC-23	*rpl14-rpl16-rps3-rps19-rpl2-rpl23*	79072 - 85227	4,567 (74.2)
GC-24	*ycf2*	85228 - 91848	5,772 (87.2)
GC-25	**trn*E, **trn*L2, **trn*M	91849 - 92152	303 (-)
GC-26	*ndh*B	92153 - 95069	2,225 (76.3)
GC-27	*3'rps12-rps7*	95070 - 96289	468 (29.1)
GC-28	*16S-23S-4.5S-5S ribosomal RNA*	96290 - 106075	4,524 (46.2)
GC-29	*ycf1-rps15-ndh*H-*ndh*A-*ndh*I-*ndh*G	106076 - 117316	10,216 (90.9)
GC-30	*ndh*E-*psa*C-*ndh*D	117317 - 119928	2,046 (78.4)
GC-31	*ccs*A	119929 - 121207	972 (76.1)
GC-32	**trn*M, **trn*L1, **trn*Q, **trn*W	121208 - 121897	689 (-)

[1]Coding percentage (%) was calculated as the proportion of gene length compared to the total length of the LCB.

[2]The plastid genome of *Cicer arietinum* was used as a reference.

452 Table 3. Reversal distance matrix, produced by GRIMM, between each major plastotypes
453 (see Fig. 2b).

	a	**b**	**c**	**d**	**e**	**f**	**g**	**h**	**i**	**j**	**k**	**l**	**m**	**n**
a	0	5	3	5	2	7	4	6	5	6	7	10	7	8
b		0	8	8	7	12	9	11	10	11	10	15	12	13
c			0	8	5	10	7	9	8	9	10	13	10	11
d				0	5	10	7	9	8	9	8	13	10	11
e					0	7	4	6	5	6	7	10	7	8
f						0	5	9	8	9	10	13	10	11
g							0	6	56	30	7	10	7	8
h								0	1	4	5	8	5	6
i									0	3	4	7	4	5
j										0	1	4	1	2
k											0	5	2	3
l												0	3	4
m													0	1
n														0

454

411 ## Figure legends

412 Figure 1 –Example of rearrangements and reversal distances between plastid genomes. A
413 comparison of the order and orientation of locally collinear blocks (LCBs) among four
414 species: *Cicer arietinum, Lens culinaris, Trifolium strictum* and *Lathyrus clymenum*. LCBs
415 are represented as differently coloured boxes and the numbers refer to the LCB IDs in Table
416 2. Inverted LCBs are positioned on an inner circle. Reversal distances (see Material and
417 Methods) between species is shown on arrowed lines. Two plastid inversion events between
418 *C. arietinum* and *L. culinaris* are highlighted.

419

420 Figure 2 – Plastid rearrangements of the investigated species shown in a phylogenetic
421 context. (a) A cladogram showing the phylogenetic relationship among the species in this
422 study. The phylogeny was constructed from a concatenated alignment of plastid protein
423 coding genes. All nodes except one were retrieved with a 100% bootstrap support. (b) Visual
424 representation of the rearranged plastid genomes of the species in this study. Locally
425 collinear blocks (LCBs) are represented as coloured boxes. The letter in the middle of each
426 circle refers to the major plastotype of each species, shown after the species names in
427 parenthesis in the cladogram (a).

428

429 Figure 3 – The relationship between the pairwise species divergence and the reversal distance
430 of the plastid genome analysed in this study. Synomyous substitutions rates (Ks) of plastid
431 protein coding genes are used as a proxy for species divergence time, and are shown on the x-
432 axis. The reversal distance (extent of rearrangements) is shown on the y-axis. The black line
433 is a smooth curve that illustrates the relationships among these two variables. 95%
434 confidence intervals are represented as grey areas around the line.

435

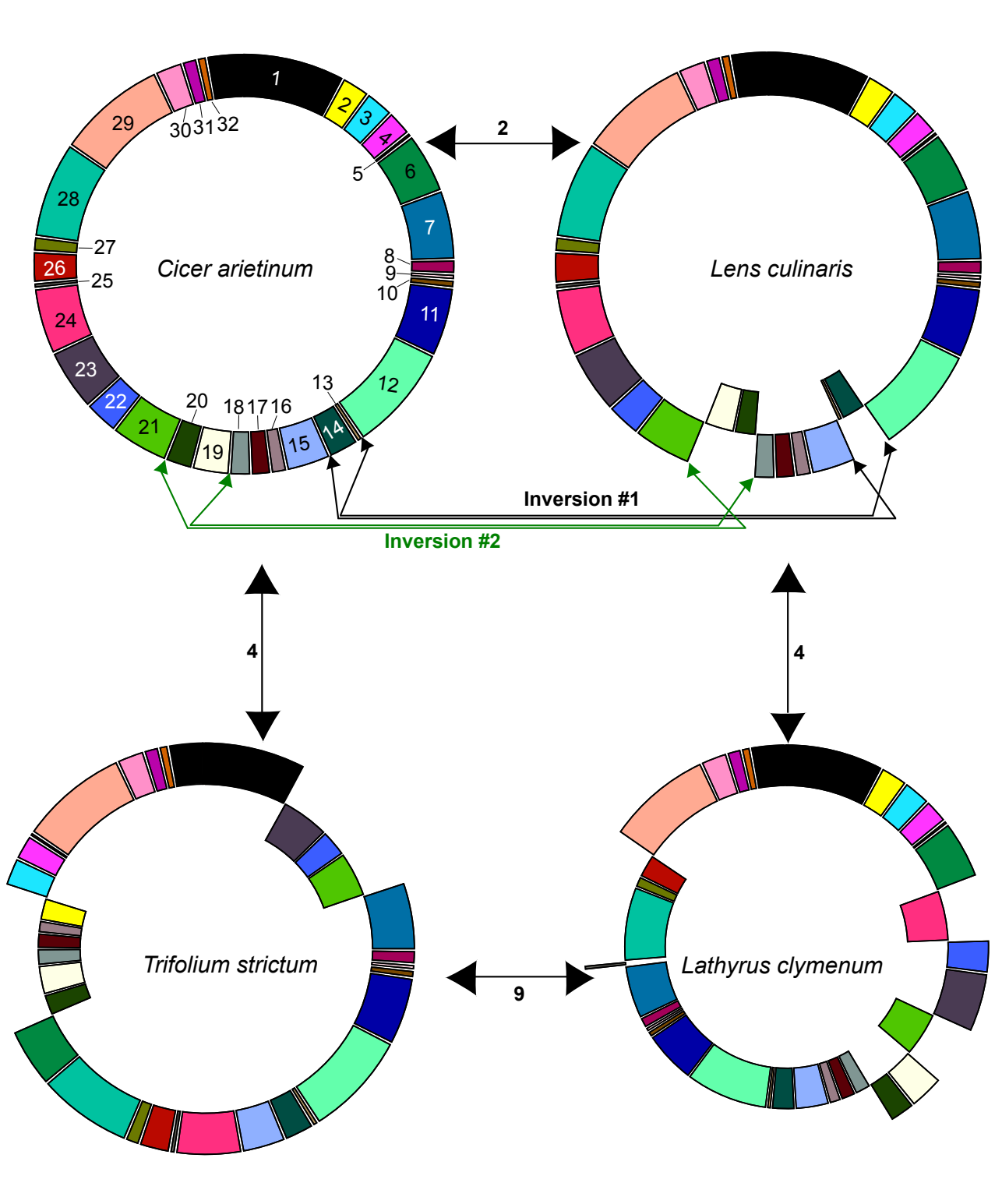
Cicer arietinum
Lens culinaris
Trifolium strictum
Lathyrus clymenum
2
4
4
9
Inversion #1
Inversion #2
Legend
#
Reversal distance
Inversion event
LCB

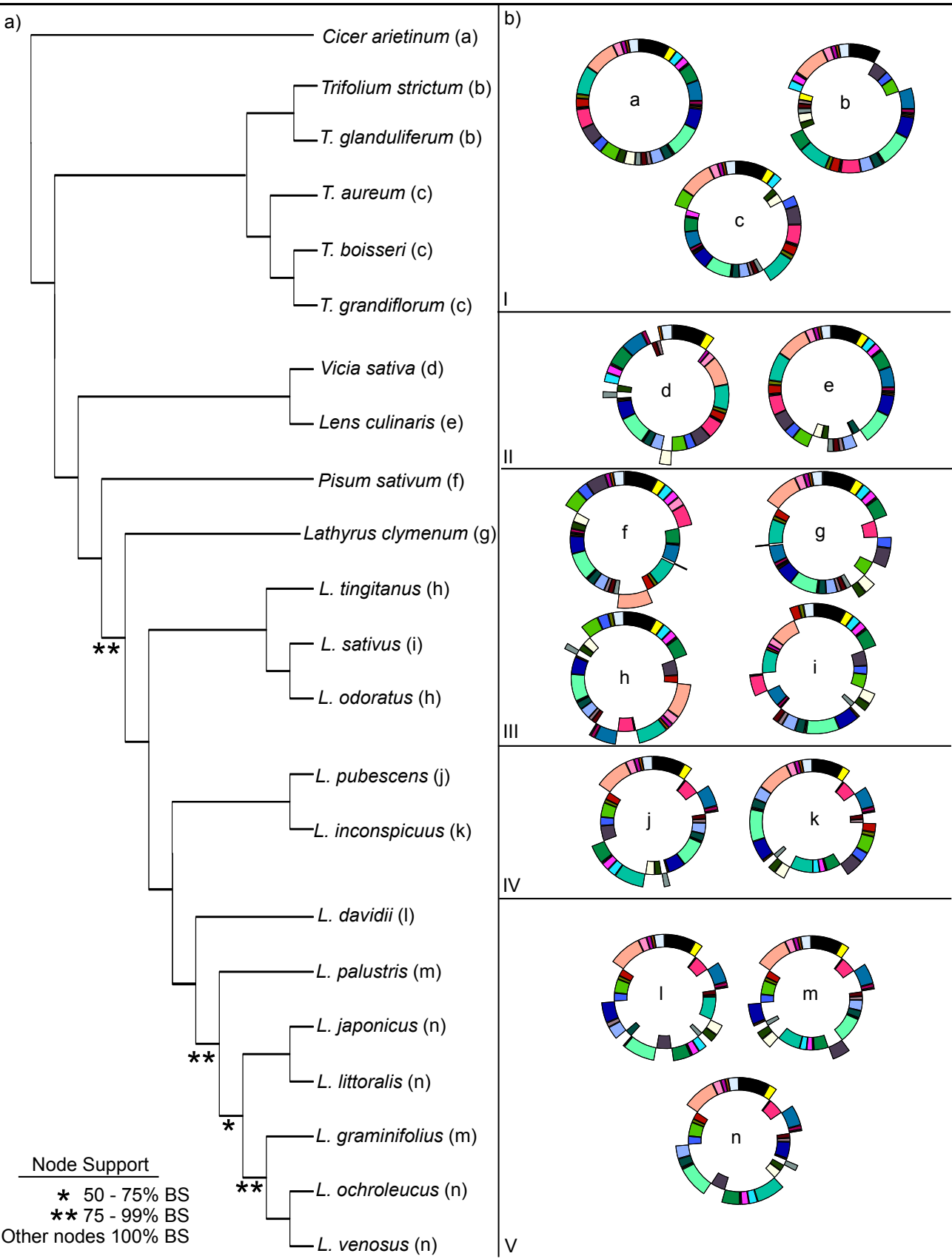
a)
Cicer arietinum (a)
Trifolium strictum (b)
T. glanduliferum (b)
T. aureum (c)
T. boisseri (c)
T. grandiflorum (c)
Vicia sativa (d)
Lens culinaris (e)
Pisum sativum (f)
Lathyrus clymenum (g)
L. tingitanus (h)
L. sativus (i)
L. odoratus (h)
L. pubescens (j)
L. inconspicuus (k)
L. davidii (l)
L. palustris (m)
L. japonicus (n)
L. littoralis (n)
L. graminifolius (m)
L. ochroleucus (n)
L. venosus (n)
**
**
*
**
Node Support
* 50 - 75% BS
** 75 - 99% BS
Other nodes 100% BS
b)
a
b
c
I
d
e
II
f
g
h
i
III
j
k
IV
l
m
n
V

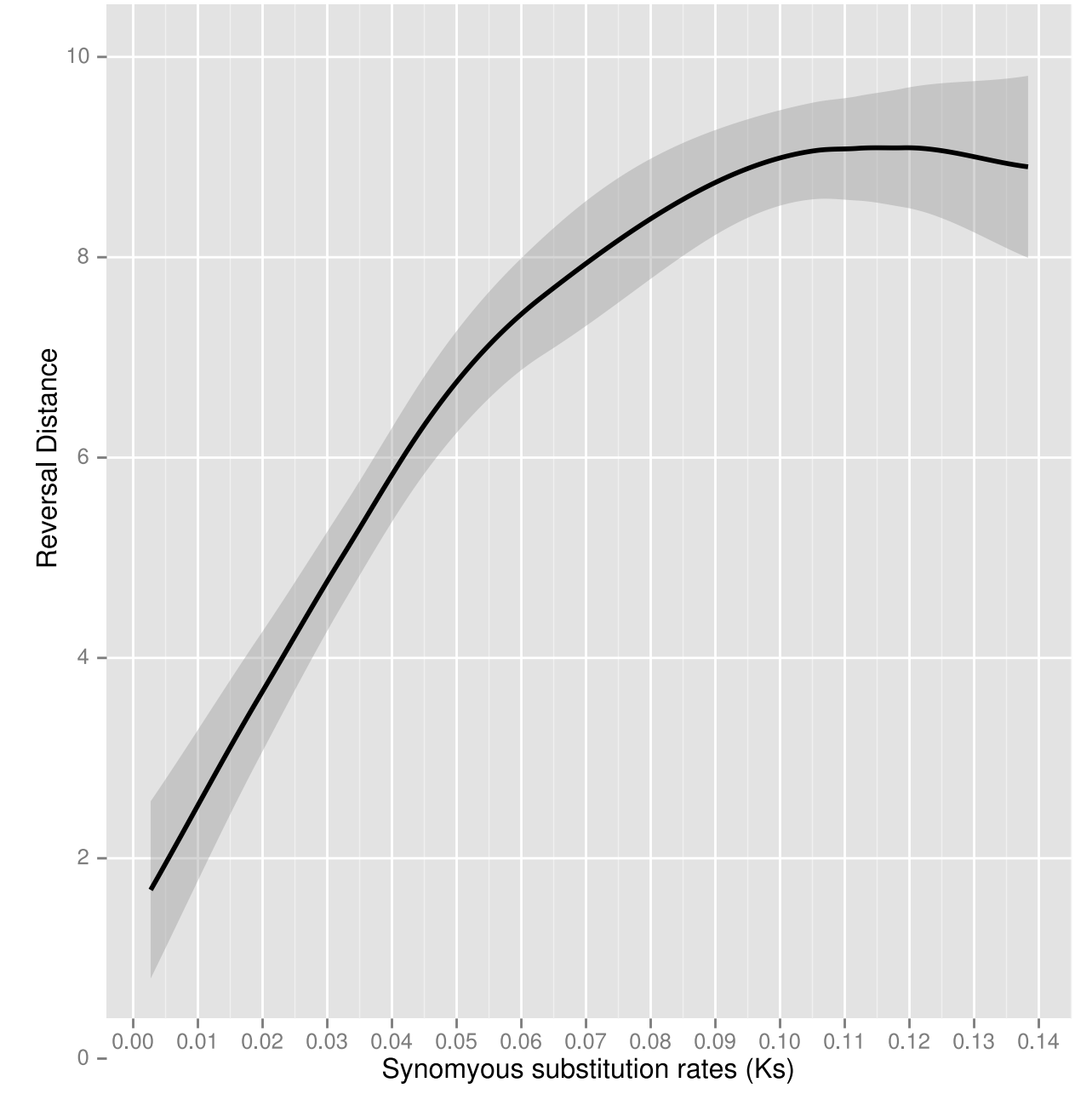
Reversal Distance
10
8
6
4
2
0
0.00
0.01
0.02
0.03
0.04
0.05
0.06
0.07
0.08
0.09
0.10
0.11
0.12
0.13
0.14
Synomyous substitution rates (Ks)